Biological Journal of the Linnean Society, 2017, **121**, 38–49. With 3 figures.

Swimming and running: a study of the convergence in long bone morphology among semi-aquatic mustelids (Carnivora: Mustelidae)

LÉO BOTTON-DIVET[1,*], RAPHAËL CORNETTE[2], ALEXANDRA HOUSSAYE[1], ANNE-CLAIRE FABRE[1] and ANTHONY HERREL[1]

[1]*UMR 7179, Muséum National d'Histoire Naturelle, Centre National de la Recherche Scientifique, Mécadev, 57 rue Cuvier, CP 55, 75005 Paris, France*
[2]*UMR 7205, CNRS / MNHN / UPMC / EPHE, Institut de Systématique, Évolution, Biodiversité (ISYEB), Muséum National d'Histoire Naturelle, 45 rue Buffon, 75005 Paris, France*

Received 19 August 2016; revised 18 October 2016; accepted for publication 2 November 2016

The shape of long bones is linked to a species' ecology and is thought to reflect the constraints imposed by locomotion. The evolution of the shape of the long bones in semi-aquatic mustelids has likely been shaped by the divergent mechanical properties of both water and land. Adaptation to a semi-aquatic lifestyle occurred independently in otters (Lutrinae) and minks (Mustelinae). Here we test the idea that these similar locomotor constraints led to morphological convergence between minks and otters, and between European and American minks. We use 3D geometric morphometrics to quantify shape differences in the humerus, radius, ulna, femur, tibia and fibula of ten species of mustelids belonging to the Lutrinae and Mustelinae subfamilies. Our results show convergence in all bones between the European and American minks, but this convergence is significant only for the humerus. We suggest that this strong convergence in humeral shape between the two minks results from functional demands on the forelimb as it produces most of the thrust when swimming in minks. The American minks show a slight but nonsignificant convergence with the Lutrinae for the shape of the ulna, femur and tibia. The sea otter (*Enhydra lutris*) shows an ulnar and radial shape that diverges from that observed in the other Lutrinae, possibly due to the strong manipulative abilities and unique locomotor mode of this species. In contrast to our initial hypothesis, bone shape in minks does not converge significantly with that of otters. Otters show a large variety of shapes suggesting that a semi-aquatic lifestyle can comprise a wide array of locomotor behaviours.

ADDITIONAL KEYWORDS: Convergence – geometric morphometrics – long bones – Mustelidae – semi-aquatic mammals.

INTRODUCTION

Bone shape evolution is impacted by functional, developmental, and architectural constraints as well as phylogenetic heritage (Chamay & Tschantz, 1972; Bass *et al.*, 2002; Andersson, 2004; Cubo, 2004; Ruff, Holt & Trinkaus, 2006; Cubo *et al.*, 2008; Morgan, 2009; Álvarez, Ercoli & Prevosti, 2013; Rose *et al.*, 2014; Fabre *et al.*, 2015). Therefore, the locomotor apparatus of a species should reflect, at least partially, a species' locomotor ecology.

*Corresponding author. E-mail: lbottondivet@mnhn.fr

Water and land induce different mechanical constrains for animal locomotion (Schmidt-Nielsen, 1972; Gillis & Blob, 2001). The differences in viscosity and density of water versus air result in differences in the forces operating on an animal moving through the two media. Whereas for terrestrial animals gravity and inertial forces dominate, in water drag-based forces form the principal constraints on locomotion. Therefore, semi-aquatic animals that move through media with strongly distinct mechanical properties should display a locomotor apparatus marked by these potentially divergent functional constraints.

Mustelidae show a great ecological diversity and diverse locomotor specializations (Schutz & Guralnick,

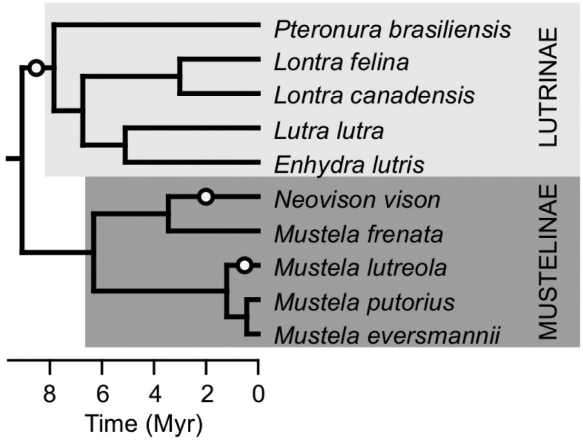

Figure 1. Phylogeny used in the study based on the tree in Slater *et al.* (2012). Black circles: shifts to a semi-aquatic lifestyle. Time scale in million years.

2007; Larivière & Jennings, 2009; Fabre *et al.*, 2015). Otters (Lutrinae) are all semi-aquatic but they live in a large variety of environments ranging from oceans to freshwater streams (Nowak, 2005; Larivière & Jennings, 2009) and spend from 20% to about 100% of time in water depending on species and food availability (Nolet & Kruuk, 1989; Beja, 1996; Larivière & Jennings, 2009). The sister group of otters, the Mustelinae (Fig. 1), encompasses two species that are considered as semi-aquatic: the European mink *Mustela lutreola* (*M. lutreola*) and the American mink *Neovison vison* (*N. vison*) (Williams, 1983a, b; Youngman, 1990; Lodé, 1999). Otters and the two minks represent three independent returns to an aquatic environment among the Musteloidea (Agnarsson, Kuntner & May-Collado, 2010; Slater, Harmon & Alfaro, 2012; Sato *et al.*, 2012). Similar to their terrestrial relatives, both minks swim mainly using forelimb paddling (Williams, 1983a, b; Lodé, 1999). Otters use swimming strategies ranging from four limb paddling to body and tail undulation depending on the species, swimming speed, and on whether they swim at the water surface or underwater (Estes, 1980; Fish, 1994; Larivière, 2001; Nowak, 2005; Larivière & Jennings, 2009). For example, *Pteronura brasiliensis* (*P. brasiliensis*) swims using quadrupedal paddling at low speed and switches to tail undulation for high-speed underwater swimming (Nowak, 2005). As they face similar locomotor environments and use the same locomotor organs, these different taxa are submitted to similar selective pressures on their locomotor apparatus. Given that the mustelids radiated three times independently into an aquatic environment, their locomotor apparatus can be expected to show convergence to a semi-aquatic mode of locomotion. On the opposite, the maintenance of terrestrial locomotion in the locomotor repertoire may prevent semi-aquatic species from evolving a different morphology. Previous studies have described morphological convergence among carnivorans, mainly focusing on skull, mandible, and dental shape and their link with feeding ecology (Van Valkenburgh, 2007; Wroe & Milne, 2007; Figueirido *et al.*, 2010; Meloro, Clauss & Raia, 2015). Nevertheless only a few studies provide quantitative tests for morphological convergence (e.g. Stayton, 2006, 2015; Mahler *et al.*, 2013). In general, convergence in the locomotor apparatus has received only little attention to date. Hence, the aim of this study is: (1) to test for potential convergence in the morphology of the long bones of both the fore- and hind limbs between the two minks, and between each mink and the otters; (2) to discuss the functional implications of these convergences.

MATERIAL AND METHODS

Materials

We selected five species of Mustelinae and five species of Lutrinae on the basis of their ecological diversity (terrestrial, marine, and freshwater environments) and their availability in zoological collections. For each species two to six specimens were used depending on their availability in collections (Table 1). To compare with the semi-aquatic *N. vision*, its sister taxon *Mustela frenata* (*M. frenata*) was selected. *M. frenata* is a terrestrial mustelid, inhabiting environments ranging from alpine to tropical (Sheffield & Thomas, 1997). To compare with the semi-aquatic *M. lutreola*, the terrestrial Mustela putorius (*M. putorius*) and Mustela eversmannii (*M. eversmannii*) were selected. These three species are morphologically similar (Blandford, 1987; Lodé, 1999), *M. lutreola* being only slightly smaller than the other two (Larivière & Jennings, 2009). *M. putorius* and *M. eversmannii* differ in habitat preference (Blandford, 1987). Whereas *M. putorius* can be found in a very wide range of environments, such as forest, marshes, and agricultural areas, *M. eversmannii* avoids densely vegetated areas (Hunter & Barrett, 2011). Therefore, *M. lutreola, M. putorius,* and *M. eversmannii* constitute a gradient from semi-aquatic to completely terrestrial species.

Terrestrial Mustelinae constitute the closest extant terrestrial relatives of the Lutrinae. We selected five species of otters: *Enhydra lutris (E. lutris)*, the sea otter, which is the most aquatic species of all extant otters and lives in a marine environment; *Lontra felina*, the marine otter, which is also attached to marine environment; *Lontra canadensis*, the American river otter; *Lutra lutra*, the Eurasian otter that can be found in both freshwater and marine environments; and *P. brasiliensis*, the giant otter, a large sized freshwater species, which displays a flattened tail.

Table 1. Specimens, bones, and body mass for species used in this study

Subfamily	Species	Specimen collection numbers and bones sampled	Body mass (kg)	Environment
Lutrinae	*Enhydra lutris*	MNHN 1935-124, MNHN A12503, UAM 21898, UAM 21978, UAM 21980, UAM 21988	29	Marine
Lutrinae	*Lontra canadensis*	UAM 53927, UAM 53928[h], UAM 67696	8.3	Freshwater/ marine
Lutrinae	*Lontra felina*	MNHN 1884-872,MNHN 1884-873[hur], MNHN 1884-874, MNHN 1995-185[h]	4.5	Marine
Lutrinae	*Lutra lutra*	MNHN 1996-2466[h], MHNB 10351, MHNB 10928, MHNB 9230	9.5	Freshwater/ marine
Lutrinae	*Pteronura brasiliensis*	MNHN 1937-889[hf], MNHN A1918, SMNS 1300	27	Freshwater
Mustelinae	*Mustela eversmannii*	MNHN 2005-668, MHNB 8546, ZMB 12407	1.7	Terrestrial
Mustelinae	*Mustela frenata*	MCZ 61107, MCZ 61285, MCZ 61322, MCZ 61328, MCZ 63641	0.26	Terrestrial
Mustelinae	*Mustela lutreola*	MNHN 1962-332, MNHN 1987-177, MNHN 1986-458[ub], MNHN 1962-288, MHNB CIII808	0.75	Freshwater
Mustelinae	*Mustela putorius*	MNHN 1991-605, MNHN 2004-639, MNHN 1997-440, MNHN 2004-311, MNHN 1972-627	1.1	Terrestrial
Mustelinae	*Neovison vison*	MCZ 61107, MCZ 61285, MCZ 61322, MCZ 61328, MCZ 63641, MNHN 1958-165	1.1	Freshwater

Note: Absent bones: [h] humerus, [u] ulna, [r] radius, [f] femur, [t] tibia, [b] fibula. Body mass and environment from Larivière & Jennings (2009).
Institutions abbreviations: MNHN, Museum National d'Histoire Naturelle, Paris; NMNH, National Museum of Natural History, Washington; MCZ, Museum of Comparative Zoology, Harvard; UAM, University of Alaska Museum, Fairbanks; ZMB, Museum fur Naturkunde, Berlin; MHNB, Naturhistorisches Museum Basel; SMNS, Staatliches Museum für Naturkunde Stuttgart.

We studied the humerus, ulna, radius, femur, tibia and fibula from the left side in all specimens when available; otherwise bones from the right side were selected and digitized bones were mirrored prior to analysis. The ontogenetic stage of the specimens was estimated on the basis of epiphysis fusion and those identified as juveniles were excluded from the analysis. Bones showing abnormal bone accretion or uncommon articular surface wear were also removed. As long bone osteological preparations are rare for some species, we decided to use both males and females, depending on their availability. See Table 1 for details on specimens and their origin.

METHODS

Bone digitization

Bones were digitized in three dimensions using a white light fringe Breuckmann 3D surface scanner (white light fringe StereoSCAN[3D] model with a camera resolution of five megapixels).

Morphometrics

Since long bones show only a few anatomical landmarks, it is impossible to describe the whole bone using anatomical landmarks only. Consequently semi-landmarks sliding on both curves and surfaces were used. This procedure is detailed in Gunz, Mitteroecker & Bookstein (2005) and allows one to build a spatially homologous landmarks set. The details of the landmarks, their location, and the number and repartition of semi-landmarks on each bone are given in the supporting information (Table S1).

Landmarks and curves were digitized on the surface of the scans using the IDAV Landmark software package (Wiley *et al.*, 2005). Curve sliding semi-landmarks were equidistantly re-sampled using the algorithm given in Botton-Divet *et al.* (2016). All curves are bordered by anatomical landmarks as recommended by Gunz, Mitteroecker & Bookstein (2005). The repeatability of anatomical landmarks was estimated on measurements taken five times on each of the five *M. frenata* specimens. This landmark set was superimposed using

a Generalized Procrustes Analysis (GPA; Gower, 1975; Rohlf & Slice, 1990) and the results visualized through a Principal Component Analysis (PCA, see Supporting information, Figs S1 and S2). Inter-measurement variability was visually estimated to be much smaller than inter-specimen differences.

For each of the six bones, points were manually placed on the surface of a template specimen mesh using the IDAV Landmark software package. This template was used for the projection of surface sliding semi-landmarks onto the surface of the specimens using the 'placePatch' function of Morpho package (Schlager, 2013). Semi-landmarks were slid on the curves and surfaces of the bone in order to minimize the bending energy of a thin plate spline (TPS) deformation of a common reference. As recommended by Gunz & Mitteroecker (2013), the template was used as a common reference for the first sliding step, and then the Procrustes consensus was used as a reference during the next three iterative steps. Sliding semi-landmarks were slid using the package 'Morpho' (Schlager, 2013) in the R environment (R Core Team, 2014) as detailed in Botton-Divet *et al.* (2015).

As our study focuses on between species convergence, we used species means. To do so a first GPA was performed for each species. Subsequently the Procrustes consensus obtained for each species was used as the representative of the species. To pool all species in a single morphospace, the Procrustes consensus of each species obtained during the first GPA were superimposed in second GPA. All GPAs were performed using the Rmorph package (Baylac, 2013).

Then distributions of superimposed datasets were visualized by performing PCA on superimposed coordinates projected onto the tangent space. Shapes associated with both sides of the PCA axes were computed and used to constrain a TPS deformation of the template mesh using the 'Morpho' R package for visualization purpose.

Statistics

To test for convergence between the two minks and between minks and otters, we used the convergence measures described in Stayton (2015). Quantitative shape descriptors permit the description of convergence by quantifying the reduction in the phenotypic distance between two taxa when compared to the maximal distance between their ancestors. For pairs of taxa we computed the percentage of convergence (C1) that 'represents the proportion of the maximum distance between two lineages that has been "closed" by subsequent evolution' (Stayton, 2015), the convergence distance (C2), the proportion of convergence (C1) over the total phenotypic evolution along the lineage between hypothetically convergent taxa and their most recent common ancestor (C3), and the proportion of convergence (C1) over the total phenotypic evolution among the clade defined by the most recent common ancestor of the two tested taxa (C4). These metrics were computed using a function derived from the 'convrat' function of the 'convevol' (Stayton, 2014) package (Supporting information, Appendix S3). To assess significance of these values we used the 'convratsig' function of the same package with 10 000 iterations. This test computes C1, C2, C3, and C4 of phenotypic values on a given tree using a Brownian motion model constrained by the covariance matrix of the landmark data. Then the function measures the frequency of simulated C1, C2, C3, and C4 with values greater or equal to the observed values. If the frequency is less than 5%, the hypothesis of convergence resulting from random evolution is rejected. Tests for convergence between the European mink and the Lutrinae, and between the American mink and the Lutrinae, were performed by computing the shape of the Lutrinae common ancestor using the 'multianc' function of the 'convevol' R package. Then we tested for convergence between each mink and the ancestor as recommended in Stayton (2015). The phylogeny used for convergence testing was derived from Slater *et al.* (2012) by pruning down the tree to the taxa included in this study.

As it is known that animal size affects bone shape (Christiansen, 2002; Fabre *et al.*, 2013), we used body mass as an indicator of animal size to evaluate the effect of the animal size on bone shape. We obtained mean species body mass data from the literature (Larivière & Jennings, 2009). Correlations between the PCA axes and the Log_{10} transformed body mass of the animals were tested using Pearson's product moment correlation implemented in the 'stats' package in R.

We then tested for convergence between the aforementioned three pairs when correcting for allometric effects. To do so we regressed the species coordinates in the tangent space onto the Log_{10} of the body mass (see Supporting information, Table S1) and tested the convergence among residuals.

RESULTS

The PC scores of species on the first principal component (PC) axis of the humerus, radius, femur, tibia, and fibula and the second PC axis of the ulna are significantly correlated with body mass (Table 2).

Principal components analyses

Forelimb bones

The two first axes of the PCA on the humerus shape data (Fig. 2A) represent 78.7% of the total variance.

Table 2. Correlation between PC scores of per species centroid and body mass (Log_{10}) of the corresponding species and test of this correlation using Pearson's product-moment correlation. Bold: significant

		R	*T*	d.f.	*P*-value
Humerus	**PC1**	**0.97**	**10.86**	**8**	**<0.01**
	PC2	0.05	0.13	8	0.90
Ulna	PC1	0.45	1.43	8	0.19
	PC2	**0.76**	**3.36**	**8**	**<0.01**
Radius	**PC1**	**–0.84**	**–4.37**	**8**	**<0.01**
	PC2	–0.46	–1.46	8	0.18
Femur	**PC1**	**0.97**	**10.47**	**8**	**<0.01**
	PC2	0.07	0.20	8	0.85
Tibia	**PC1**	**0.97**	**10.58**	**8**	**<0.01**
	PC2	0.08	0.24	8	0.82
Fibula	**PC1**	**–0.94**	**–7.92**	**8**	**<0.01**
	PC2	0.10	0.26	8	0.81

The first axis separates Mustelinae (negative side of the axis) and Lutrinae (positive side of the axis). The three closely related *Mustela* species *M. lutreola*, *M. putorius* and *M. eversmannii* are spread along the second axis. The two minks *M. lutreola* and *N. vison* are positioned close to one another, together with *M. frenata* (see Supporting information, Fig. S3A). The deformations associated with positive scores on the first axis are: more robust bones with expanded epiphyses; more curved diaphysis around its middle with an expansion of the cranial side between the greater trochanteric crest and the deltoid crest, and a larger capitulum (Fig. 3A). The shapes on the positive side of the second axis are: a more curved humerus with the maximal curvature being more proximal, a humeral head that is less elongated antero-posteriorly, and consequently more round and a narrower capitulum.

The two first axes of the PCA on the ulna shape data (Fig. 2B) represent 80% of the total variance. The first axis separates *E. lutris* and *P. brasiliensis*. The second axis of the PCA separates the largest Lutrinae species *E. lutris* and *P. brasiliensis* on the positive side from the Mustelinae on the negative side. The two sub-families separate when taking the first two PC axes into account. *N. vison* and *M. lutreola* are close to each other (see Supporting information, Fig. S3B), but the spread of the Mustelinae in the morphospace is smaller than that of the Lutrinae. *N. vison* tends to separate from *M. frenata* and come closer to the otters. Specimens with high scores on the first axis show a robust ulna with a long olecranon process expanding towards the caudo-medial direction and a widely opened trochlear notch (Fig. 3B). The second axis separates specimens with a square olecranon, a cranially expanded medial coronoid process, and a robust distal half of the ulna on the positive side of the axis from specimens with a round caudal margin of the olecranon and a distally curved diaphysis.

The two first axes of the PCA on the radius (Fig. 2C) account for 79.3% of the total variance. The first axis separates the Lutrinae on the negative side from the Mustelinae on the positive one. The second axis separates *E. lutris* from the other species. *N. vison* and *M. lutreola* are positioned close to each other (see Supporting information, Fig. S3C), but the spread of the Mustelinae in the morphospace is small as compared to that of Lutrinae. *N. vison* tends to separate from *M. frenata* and move closer to the otters. Species with low scores on the first axis of the radius PCA have a more robust radius (Fig. 3C). Their diaphysis is expanded on the distal part at the latero-cranial side and the epiphyses are larger. The radial tuberosity is located more distally. The second axis separates specimens with a round proximal epiphysis on the negative side from specimens with an oval proximal epiphysis with a more laterally curved diaphysis.

Hind-limb bones

The three hind-limb long bones show similar PCA patterns. The first axis differentiates the Mustelinae from the Lutrinae whereas the second axis is driven by the diversity among the Lutrinae. The two first axes of the PCA account for 89.7% of the total variance for the femur (Fig. 2D), 81.6% for the tibia (Fig. 2E), and 73.7% for the fibula (Fig. 2F). For femur, tibia, and fibula, *M. lutreola* and *N. vison* are positioned close to one another in the morphospace (see Supporting information, Fig. S3D–F). The shape of the femur and tibia of the *N. vison* tends to separate it from *M. frenata* and be more similar to that of the otters.

The first axis of the PCA on the femur separates specimens with a robust femur with large and wide epiphyses on the positive side of the axis from specimens with a gracile femur with relatively small epiphyses on the negative side (Fig. 3D). Specimens with low scores on the second axis tend to possess a more curved diaphysis, and a femoral neck forming an obtuse angle with the diaphysis.

Specimens with high scores on the first axis of the PCA on tibia show wide epiphyses leading to a laterally curved tibia (Fig. 3E). Specimens with low scores tend to display a point of antero-posterior curvature that lies more proximal. Specimens with high scores on the second axis display a double antero-posterior curvature forming an 'S' shape whereas specimens with low scores show a single curvature oriented cranially.

The first axis of the PCA on fibula separates specimens with large epiphyses on the negative side from specimens with narrow epiphyses (Fig. 3F). The second

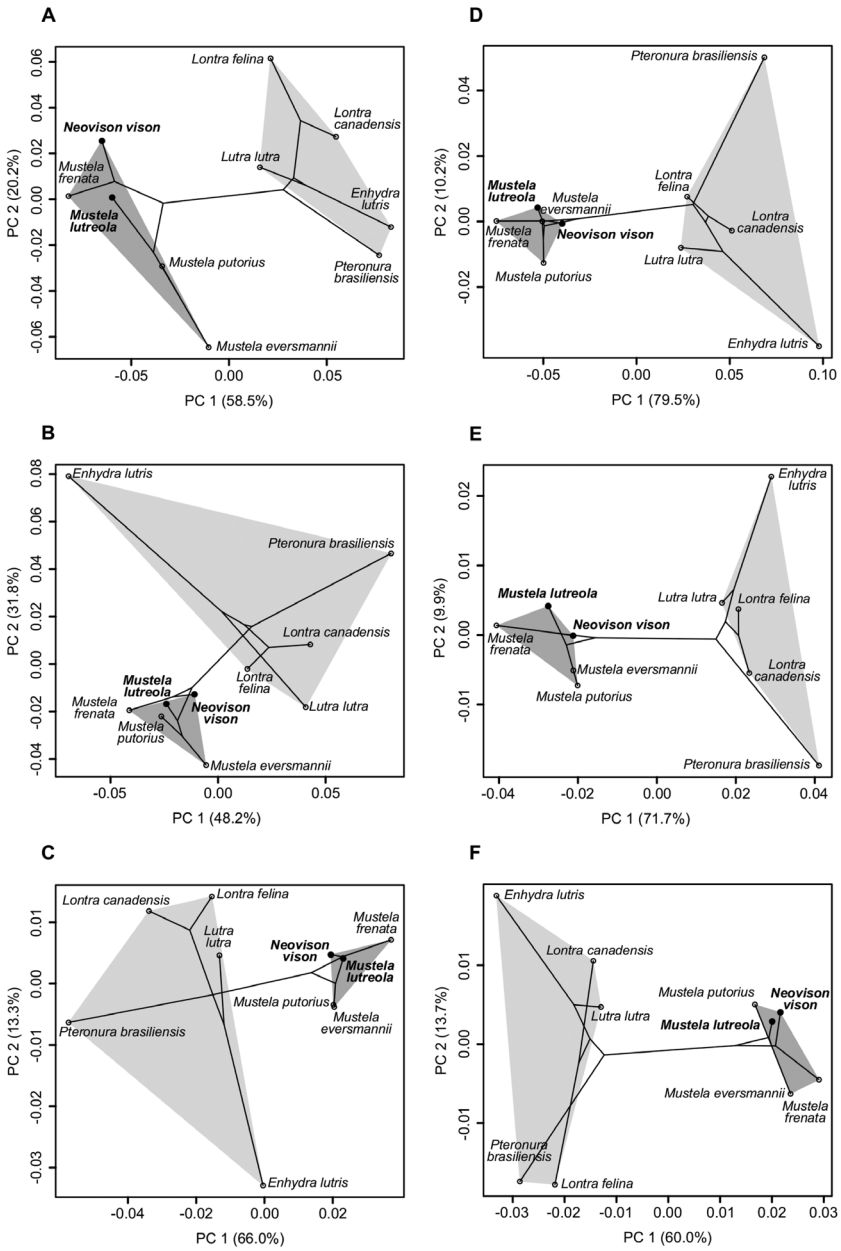

Figure 2. Principal component analysis of morphometric data per bone. Phylogeny is represented in the morphospace. Area in light grey represent Lutrinae, area in dark grey represent Mustelinae. In bold focal species of this study. A: humerus; B: ulna; C: radius; D: femur; E: tibia; F: fibula.

axis separates specimens with a laterally expanded malleolus and straight diaphysis on the negative side from specimens with a lateral curvature and a short malleolus on the positive one.

Convergence

For all six bones, the two minks are located in the same area of the morphospace regardless of where their terrestrial relatives are located (Fig. 2). To test for convergence between the two minks we performed distance based convergence tests (Stayton, 2015). Values of the convergence metrics and the corresponding *P*-values are reported in Table 3. The two minks exhibit convergent shapes for all bones, though only the convergence of the humerus is significant (Table 3). The shape of the ulna, femur, and tibia of *N. vison* shows convergence with that of the Lutrinae but the hypothesis of a convergence resulting from random evolution cannot be excluded. For the humeral

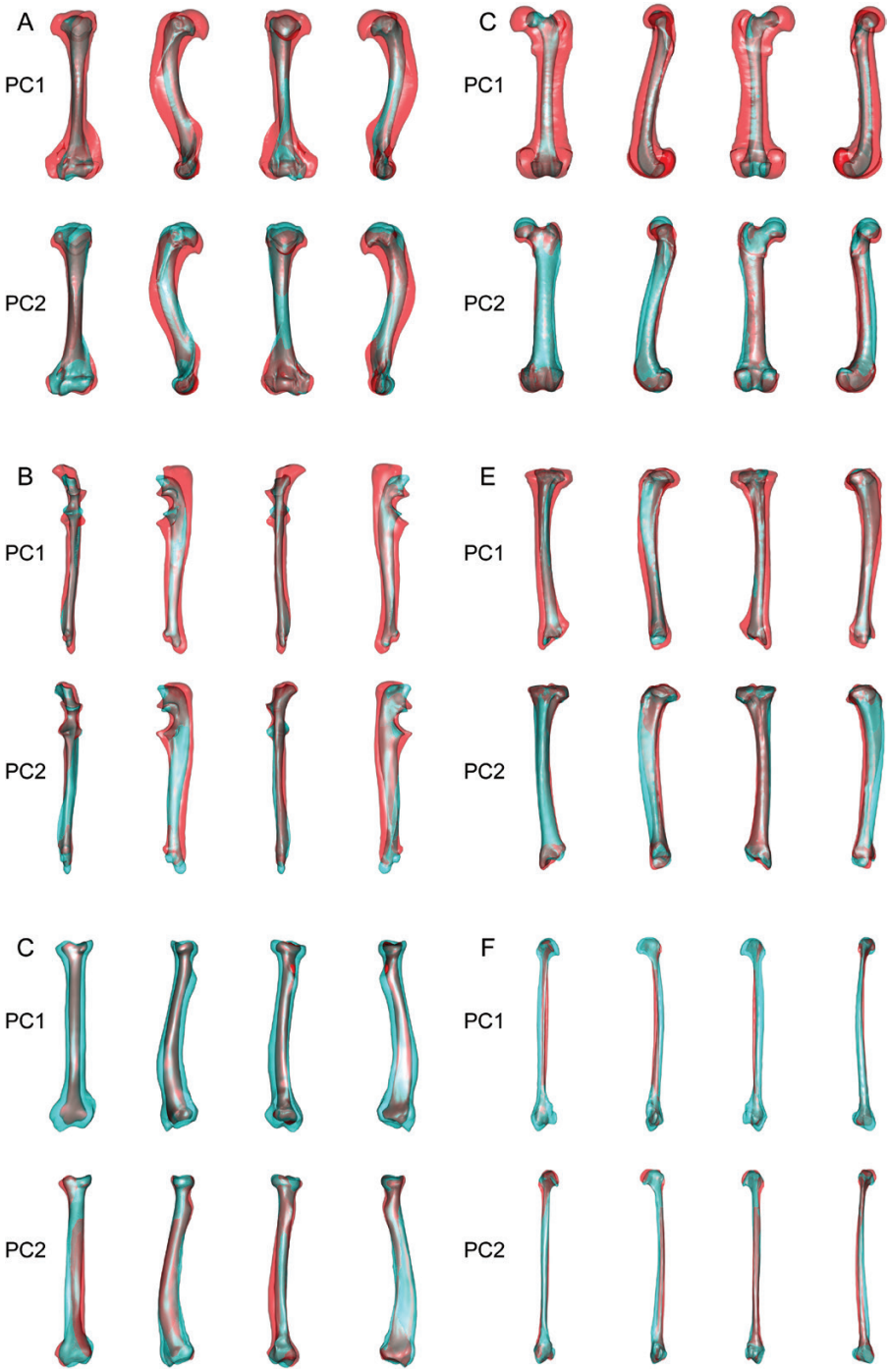

Figure 3. Deformations associated with the two first PCs of each bone. A: humerus; B: ulna; C: radius; D: femur; E: tibia; F: fibula. In blue deformations associated with the low score on the axis; in red deformations associated with the high scores on the axis. Bone orientation from left to right: caudal, lateral, cranial, and medial.

shape, the two minks show 43% of convergence, which represents 22% of the total phenotypic evolution of this lineage, and 11% of the total phenotypic evolution in the clade proceeding from their most recent common ancestor.

The shape of the humerus of the two minks converges mainly on the second axis of the PCA (Fig. 2A). When compared to their ancestors, they tend to display a more curved and laterally flattened diaphysis (Fig. 3A). The lesser trochanter tends to expand more distally and

Table 3. Convergence metrics and associated *P*-values for each bone for the two minks (*Mustela lutreola* and *Neovison vison*), and each mink versus the Lutrinae common ancestor (ancestral state reconstruction). Bold: significant

		C1	*P*-value	C2	*P*-value	C3	*P*-value	C4	*P*-value
M. lutreola / *N. vison*	**Humerus**	**0.43**	**<0.01**	**2.6e-2**	**0.02**	**0.22**	**<0.01**	**0.11**	**0.02**
	Ulna	0.03	0.36	7.0e-4	0.41	0.01	0.40	<0.01	0.41
	Radius	0.18	0.12	2.8e-3	0.26	0.06	0.24	0.03	0.28
	Femur	0.30	0.10	9.6e-3	0.25	0.13	0.20	0.06	0.26
	Tibia	0.29	0.06	5.5e-3	0.16	0.12	0.13	0.06	0.17
	Fibula	0.24	0.06	3.8e-3	0.16	0.09	0.14	0.04	0.19
N. vison / *Lutrinae*	Humerus	0	1	0	1	0	1	0	1
	Ulna	0.08	0.23	3.9e-3	0.19	0.07	0.21	0.02	0.22
	Radius	0	1	0	1	0	1	0	1
	Femur	0.05	0.33	3.7e-3	0.29	0.04	0.32	0.02	0.31
	Tibia	0.03	0.31	1.2e-3	0.29	0.03	0.31	0.01	0.30
	Fibula	0	1	0	1	0	1	0	1
M. lutreola / *Lutrinae*	Humerus	0	1	0	1	0	1	0	1
	Ulna	0	1	0	1	0	1	0	1
	Radius	0	1	0	1	0	1	0	1
	Femur	0	1	0	1	0	1	0	1
	Tibia	0	1	0	1	0	1	0	1
	Fibula	0	1	0	1	0	1	0	1

the humeral head is laterally compressed whereas it is rounder in their ancestors. The lateral epicondylar crest starts more distally on the diaphysis and expands more laterally and caudally on its distal part. The capitulum tends to be broader than in their ancestors and the medial epicondyle tends to expand more medially.

Additionally, the shape of the humerus of minks separates from that of their ancestors by a vector pointing towards the same direction (left top corner of the Fig. 2A). Similarly, we can notice that the shape of the fibula of the two minks separates from that of their ancestors by a shift towards the same direction (right top corner; Fig. 2F), but their convergence is not significant (Table 3).

The convergence in the humerus shape between *N. vison* and *M. lutreola* remains significant when corrected for allometric effects. *N. vison* does not show any convergence with Lutrinae, however, when size is taken into account. The bone shape of *M. lutreola* tends to converge with that of the Lutrinae for all bones, but it is only significant for the humerus and femur.

DISCUSSION

Body mass

The first PCA axis of the humerus, radius, femur, tibia, and fibula and the second PCA axis of the ulna are correlated with body mass (Table 2). These axes represent from 30% up to almost 80% of the total variance of the dataset, suggesting a strong impact of size on the shape changes across the dataset. However, the otters are larger in size and body mass than the Mustelinae and more robust bones are therefore expected in Lutrinae. Therefore, the slight convergence observed between *N. vison* and the Lutrinae for the ulna, femur, and tibia could be driven by allometric effects which is confirmed by the disappearance of this convergence when tested on data corrected for allometry (Supporting information, Table S1). Nevertheless, size was shown to play a functional role in aquatic warm-blooded animals. As thermal conductivity of the water is higher than that of air, heat loss is higher in water (Dejours, 1987). Considering that the surface over volume ratio decreases when size increases, the cost of maintaining body temperature decreases when animal gets larger. This implies a very high metabolic cost for being small in an aquatic environment and therefore a lower limit for aquatic animal size (Downhower & Blumer, 1988; King, 1989; Clauset, 2013). In the mustelids, the effect of this constraint is increased by the long and thin body shape of the Mustelidae (Brown & Lasiewski, 1972). This leads to a heat loss exceeding the metabolic heat production in *N. vison* (Williams, 1986). Therefore, size changes in this group could have been driven by a heat conservation constraint, and

the bone shape changes could be driven by associated allometric effects. In addition, the very similar pattern observed for all bones sustains the strong impact of body mass on bone shape in Mustelidae (Fabre *et al.*, 2013). Nevertheless, the analyses of size free residuals suggest that at least part of the convergence in shape observed is not size related, and therefore suggests that an adaptation to a semi-aquatic lifestyle induces additional bone shape changes.

Lutrinae versus Mustelinae

Otters show more robust bones than Mustelinae. This is in accordance with the results of previous studies (Samuels, Meachen & Sakai, 2013; Fabre *et al.*, 2015). In addition to a mechanical role of body weight support during terrestrial locomotion, this increase in bone robustness could be associated with a ballast role if associated with increased inner bone compactness as suggested by Fish & Stein (1991) and Nakajima & Endo (2013).

The morphospace of the ulna and radius show very similar patterns (Fig. 3B and C). The main difference is an inversion between the first and second axes. This inversion may be explained by the fact that *E. lutris* exhibits a very divergent ulnar shape. Indeed this species displays a more slender ulna than species of similar size (*P. brasiliensis*). Additionally it has a shorter and straighter olecranon process. The very divergent shape of the forearm in *E. lutris* could be related to the unique behaviour involving the use of its forepaws for food manipulation and processing (Hall & Schaller, 1964; Howard, 1973; Estes, 1980; Bodkin, 2001; Fujii, Ralls & Tinker, 2015; Botton-Divet *et al.*, in press).

Except for the humerus, the area of the morphospace occupied by the Mustelinae is much smaller than the one occupied by the Lutrinae in PCAs (Fig. 2). This difference in shape diversity could reflect a difference in functional diversity. While locomotor patterns are highly conserved among Mustelinae (Williams, 1983a, b; Lodé, 1999), the Lutrinae show various swimming strokes depending on the species (Tarasoff, 1972; Taylor, 1989).

Convergence

The two minks appear in the same area of the morphospace for all bones studied (Fig. 2). Minks are not isolated from other Mustelinae, but their position in the morphospace is similar for all bones whereas their proximity to the other species varies. Even if the American mink (*N. vison*) is said to be a better swimmer than the European mink (Youngman, 1990), they tend to display very similar long bone shapes. All the bones are convergent between the two minks, but only the convergence in the humerus was significantly greater than what could have occurred by random evolution. The humerus presents 43% of convergence (C1) while it goes down to between 30 and 18% for the radius and hind-limb bones and down to 3% for the ulna. This suggests a stronger functional constraint on the humerus than on other bones. Minks swim using a four limb paddling, similar to the gait used for terrestrial locomotion (Williams, 1983b; Lodé, 1999). Nevertheless, these authors suggested that the forelimbs are the main thrust producers as the hind limbs move at a slower rhythm and sometimes move out of phase or even stop moving while swimming. Therefore, the convergence of the shape of the humerus could be linked to functional requirements induced by aquatic locomotion.

M. lutreola presents bone shapes that are convergent with those of the Lutrinae when we consider the size-corrected data. As this species is slightly smaller than its terrestrial relatives, convergence in the data when corrected for this size effect suggests that the allometric effect for this species is smaller than expected by the difference in body mass. This implies that the shape of the long bones in *M. lutreola* is closer to that of the Lutrinae than could be expected if this species showed scaling similar to other species. Our investigation of the details of allometric trends and directions is nevertheless limited by the size of our sample.

The accuracy of the convergence measures relies, amongst others, on the accuracy of the ancestral state reconstruction (Stayton, 2015). Adding additional supplementary species to the clades used in this study could modify the position of reconstructed ancestors in the morphospace and therefore the estimates of convergence. Therefore, future work could benefit from the inclusion of extinct species as the sea mink *Neovison macrodon* (Prentiss, 1903; Mead, Spiess & Sobolik, 2000) or the terrestrial otter *Teruelictis riparius* (Salesa *et al.*, 2013).

Biomechanical consequences of humerus shape convergence in minks

The convergence in the humeral shape of the two minks is linked with an expansion of the cranial part of the diaphysis. The area between the greater trochanter and deltoid crests is wide and expanded distally, leading to greater insertion areas of the shoulder flexor, the abductors, and the retractor including the *m. deltoideus*, the *m. pectoralis major,* and the *m. pectoralis minor* (Fisher, 1942; Howard, 1973; Ercoli *et al.*, 2014). This antero-distal displacement of the shoulder retractors implies an extended in-lever and therefore a more powerful retraction of the shoulder. When compared to terrestrial species, minks move in a dense

medium more often, and to do so they mainly use the forelimb (Williams, 1983b; Lodé, 1999). Therefore, adaptations to produce stronger shoulder movements could be linked to the mechanical requirements of paddling. The lateral epicondylar crest is wide, even if less expanded than in the Lutrinae. This crest provides origin for the *m. anconeus*, which assists elbow extension on the caudal side, and is also the origin for several digital and carpal extensors and the wrist flexor on its latero-cranial side.

N. vison tends to evolve a longer olecranon process of the ulna than its terrestrial relatives as is also observed in Lutrinae. A longer olecranon process provides a longer in-lever for the *m. triceps brachii*, an elbow extensor. Expansion of the olecranon process seems to be linked with body mass, which suggests a role for sustaining larger mechanical load during terrestrial locomotion as well. *E. lutris* shows a smaller olecranon process than other otters of similar size (*P. brasiliensis*). *E. lutris* does not use its forelimb for aquatic locomotion but also seldomly walks on land and has lost the ability to run, a feature which is maintained in all other otters (Bodkin, 2001). Additionally *E. lutris* uses its forepaws extensively to manipulate objects (Hall & Schaller, 1964; Bodkin, 2001). Consequently we cannot determine if the elongation of the olecranon is an adaptation to an increased body mass, to aquatic locomotion involving the forelimb, or to a combination of both. Thus, we cannot conclude on the functional meaning of this feature in *N. vison*.

CONCLUSION

In this study we showed that the European and the American minks have similar long bone shapes for both hind- and forelimbs. The shape of the humerus, ulna, radius, femur, tibia, and fibula of the two minks tends to converge but only the convergence of the shape of the humerus is significant. This convergence is likely the result from strong functional pressures on the forelimb of the minks as it is the principal thrust producer during swimming. The American mink tends to converge with the Lutrinae for the shape of the ulna, femur, and tibia. This convergence is in accordance with the larger size of this species. Lutrinae show robust bones and a larger diversity in all bones but the humerus compared to Mustelinae. Lutrinae display a large diversity in swimming gaits, whereas the swimming gait of Mustelinae is common to the two species and similar to their terrestrial gait. Consequently we relate the higher shape diversity in Lutrinae to their higher functional diversity. As Lutrinae display a greater shape and locomotor diversity, future investigations could try to quantify locomotor movements and muscular parameters to describe the link between bone shape, muscular anatomy, and function in relation to the semi-aquatic lifestyles of this group. Future work could benefit from the addition of extinct species, particularly terrestrial species of the otter lineage.

ACKNOWLEDGEMENTS

The authors want to thank all the collection curators for the loan of the specimens. Suzanne Peurach of the National Museum of Natural History, Washington; Judith Marie Chupasko of the Museum of Comparative Zoology, Harvard; Loïc Costeur of the Naturhistorisches Museum, Basel; Christiane Funk and Frieder Mayer of Museum für Naturkunde, Berlin; Link E. Olson and Aren Gunderson of the University of Alaska Museum, Fairbanks; Géraldine Véron, Jacques Cuisin, Julie Villemain, and Céline Bens of the Muséum National d'Histoire Naturelle, Paris; Stefan Merker of the Staatliches Museum für Naturkunde, Stuttgart. The authors would also like to thank Tristan Stayton for helping us with the convergence analyses and two anonymous reviewers who provided useful comments that really improved a previous version of this manuscript. LB-D thanks the doctoral school 'Frontières du vivant' and the Bettencourt Schueller foundation. LB-D, AIH and AnH received financial support from the ANR-13-PDOC-0011. A-CF thanks the Marie-Skłodowska Curie fellowship (EU project 655694 – GETAGRIP) for funding.

REFERENCES

Agnarsson I, Kuntner M, May-Collado LJ. 2010. Dogs, cats, and kin: a molecular species-level phylogeny of Carnivora. *Molecular Phylogenetics and Evolution* **54:** 726–745.

Álvarez A, Ercoli MD, Prevosti FJ. 2013. Locomotion in some small to medium-sized mammals: a geometric morphometric analysis of the penultimate lumbar vertebra, pelvis and hindlimbs. *Zoology* **116:** 356–371.

Andersson KI. 2004. Elbow-joint morphology as a guide to forearm function and foraging behaviour in mammalian carnivores. *Zoological Journal of the Linnean Society* **142:** 91–104.

Bass SL, Saxon L, Daly RM, Turner CH, Robling AG, Seeman E, Stuckey S. 2002. The effect of mechanical loading on the size and shape of bone in pre-, peri-, and postpubertal girls: a study in tennis players. *Journal of Bone and Mineral Research* **17:** 2274–2280.

Baylac M. 2013. *Rmorph, a morphometrics library for R*. Available from the author. baylac@mnhn.fr.

Beja PR. 1996. Temporal and spatial patterns of rest-site use by four female otters Lutra lutra along the south-west coast of Portugal. *Journal of Zoology* **239:** 741–753.

Blandford P. 1987. Biology of the polecat Mustela putorius: a literature review. *Mammal Review* **17:** 155–198.

Bodkin JL. 2001. Sea Otters. In: Steele JH, eds. *Encyclopedia of Ocean Sciences*. Oxford: Academic Press, 2614–2621.

Botton-Divet L, Cornette R, Fabre A-C, Herrel A, Houssaye A. 2016. Morphological analysis of long bones in semi-aquatic mustelids and their terrestrial relatives. *Integrative and Comparative Biology*: icw124.

Botton-Divet L, Houssaye A, Herrel A, Fabre A-C, Cornette R. 2015. Tools for quantitative form description; an evaluation of different software packages for semi-landmark analysis. *PeerJ* **3:** e1417.

Brown JH, Lasiewski R. 1972. Metabolism of Weasels: the cost of being long and thin. *Ecology* **53:** 939.

Chamay A, Tschantz P. 1972. Mechanical influences in bone remodeling. Experimental research on Wolff's law. *Journal of Biomechanics* **5:** 173–180.

Christiansen PER. 2002. Locomotion in terrestrial mammals: the influence of body mass, limb length and bone proportions on speed. *Zoological Journal of the Linnean Society* **136:** 685–714.

Clauset A. 2013. How large should whales be? *PLoS One* **8:** e53967.

Cubo J. 2004. Pattern and process in constructional morphology. *Evolution & Development* **6:** 131–133.

Cubo J, Legendre P, De Ricqlès A, , Montes L, De Margerie E, Castanet J, Desdevises Y. 2008. Phylogenetic, functional, and structural components of variation in bone growth rate of amniotes. *Evolution & Development* **10:** 217–227.

Dejours P. 1987. Water and air physical characteristics and their physiological consequences. In: Dejours P, Bolis L, Taylor CR, Weibel ER, eds. *Comparative physiology: life in water and on land*. Berlin: Springer, 3–11.

Downhower JF, Blumer LS. 1988. Calculating just how small a whale can be. *Nature* **335:** 675.

Ercoli MD, Álvarez A, Stefanini MI, Busker F, Morales MM. 2014. Muscular anatomy of the forelimbs of the lesser grison (Galictis cuja), and a functional and phylogenetic overview of Mustelidae and other Caniformia. *Journal of Mammalian Evolution*.

Estes JA. 1980. Enhydra lutris. *Mammalian Species* **133**: 1–8.

Fabre A-C, Cornette R, Goswami A, Peigné S. 2015. Do constraints associated with the locomotor habitat drive the evolution of forelimb shape? A case study in musteloid carnivorans. *Journal of Anatomy* **226:** 596–610.

Fabre A-C, Cornette R, Peigné S, Goswami A. 2013. Influence of body mass on the shape of forelimb in musteloid carnivorans. *Biological Journal of the Linnean Society* **110:** 91–103.

Figueirido B, Serrano-AlarcóN FJ, Slater GJ, Palmqvist P. 2010. Shape at the cross-roads: homoplasy and history in the evolution of the carnivoran skull towards herbivory: herbivorous adaptations in carnivores. *Journal of Evolutionary Biology* **23:** 2579–2594.

Fish FE. 1994. Association of propulsive swimming mode with behavior in River Otters (Lutra canadensis). *Journal of Mammalogy* **75:** 989.

Fish FE, Stein B. 1991. Functional correlates of differences in bone density among terrestrial and aquatic genera in the family Mustelidae (Mammalia). *Zoomorphology* **110:** 339–345.

Fisher EM. 1942. *The osteology and myology of the California river otter.* Stanford, CA: Stanford University Press.

Fujii JA, Ralls K, Tinker MT. 2015. Ecological drivers of variation in tool-use frequency across sea otter populations. *Behavioral Ecology* **26:** 519–526.

Gillis GB, Blob RW. 2001. How muscles accommodate movement in different physical environments: aquatic vs. terrestrial locomotion in vertebrates. *Comparative biochemistry and physiology. Part A, Molecular & integrative physiology* **131:** 61–75.

Gower JC. 1975. Generalized procrustes analysis. *Psychometrika* **40:** 33–51.

Gunz P, Mitteroecker P. 2013. Semilandmarks: a method for quantifying curves and surfaces. *Hystrix, the Italian Journal of Mammalogy* **24:** 103–109.

Gunz P, Mitteroecker P & Bookstein FL. 2005. Semilandmarks in three dimensions. In: Slice DE, eds. *Modern morphometrics in physical anthropology*. Ithaca, NY: Springer, 73–98.

Hall KRL, Schaller GB. 1964. Tool-using behavior of the California Sea Otter. *Journal of Mammalogy* **45:** 287–298.

Howard LD. 1973. Muscular anatomy of the forelimb of the sea otter (Enhydra lutris). *Proceeings of the California Academy of Science* **39:** 411–500.

Hunter L, Barrett P. 2011. *Carnivores of the world.* Princeton: Princeton University Press.

King CM. 1989. The advantages and disadvantages of small size to weasels, Mustela species. In: Gittleman JL , eds. *Carnivore behavior, ecology, and evolution*. Ithaca, NY: Springer, 302–334.

Larivière S. 2001. Aonyx capensis. *Mammalian Species* **671**: 1–6.

Larivière S, Jennings AP. 2009. Mustelidae (weasels and relatives). In: Wilson DE, Mittermeier RA, eds. *Handbook of the mammals of the world. Barcelona*, Lynx, 564–656.

Lodé T. 1999. Comparative measurements of terrestrial and aquatic locomotion in *Mustela lutreola and M. putorius*. *Zeitschrift fur Saugetierkunde* **64:** 110–115.

Mahler DL, Ingram T, Revell LJ, Losos JB. 2013. Exceptional convergence on the macroevolutionary landscape in Island Lizard radiations. *Science* **341:** 292–295.

Mead JI, Spiess AE, Sobolik KD. 2000. Skeleton of extinct North American Sea Mink (Mustela macrodon). *Quaternary Research* **53:** 247–262.

Meloro C, Clauss M, Raia P. 2015. Ecomorphology of Carnivora challenges convergent evolution. *Organisms Diversity & Evolution* **15:** 711–720.

Morgan CC. 2009. Geometric morphometrics of the scapula of South American caviomorph rodents (Rodentia: Hystricognathi): form, function and phylogeny. *Mammalian Biology – Zeitschrift für Säugetierkunde* **74:** 497–506.

Nakajima Y, Endo H. 2013. Comparative humeral microanatomy of terrestrial, semiaquatic, and aquatic carnivorans using micro-focus CT Scan. *Mammal Study* **38:** 1–8.

Nolet BA, Kruuk H. 1989. Grooming and resting of otters Lutra lutra in a marine habitat. *Journal of Zoology* **218:** 433–440.

Nowak RM. 2005. *Walker's carnivores of the world.* Baltimore, MD: JHU Press.

Prentiss DW. 1903. Description of an extinct mink from the shellheaps of the Maine coast. *Proceedings of the U.S. National Museum* 24: 887–888.

R Core Team. 2014. *R: a language and environment for statistical computing.* Vienna, Austria: R Foundation for Statistical Computing.

Rohlf FJ, Slice D. 1990. Extensions of the Procrustes method for the optimal superimposition of landmarks. *Systematic Biology* **39:** 40–59.

Rose J, Moore A, Russell A, Butcher M. 2014. Functional osteology of the forelimb digging apparatus of badgers. *Journal of Mammalogy* **95:** 543–558.

Ruff C, Holt B, Trinkaus E. 2006. Who's afraid of the big bad Wolff? 'Wolff's law' and bone functional adaptation. *American Journal of Physical Anthropology* **129:** 484–498.

Salesa MJ, Antón M, Siliceo G, Pesquero MD, Morales J, Alcalá L. 2013. A non-aquatic otter (Mammalia, Carnivora, Mustelidae) from the Late Miocene (Vallesian, MN 10) of La Roma 2 (Alfambra, Teruel, Spain): systematics and functional anatomy. *Zoological Journal of the Linnean Society* **169:** 448–482.

Samuels JX, Meachen JA, Sakai SA. 2013. Postcranial morphology and the locomotor habits of living and extinct carnivorans. *Journal of Morphology* **274:** 121–146.

Sato JJ, Wolsan M, Prevosti FJ, D'Elía G, Begg C, Begg K, Hosoda T, Campbell KL, Suzuki H. 2012. Evolutionary and biogeographic history of weasel-like carnivorans (Musteloidea). *Molecular Phylogenetics and Evolution* **63:** 745–757.

Schlager S. 2013. Morpho: Calculation and visualizations related to geometric morphometrics. R package version 2.4. https://github.com/zarquon42b/Morpho

Schmidt-Nielsen K. 1972. Locomotion: energy cost of swimming, flying, and running. *Science* **177:** 222–228.

Schutz H, Guralnick RP. 2007. Postcranial element shape and function: assessing locomotor mode in extant and extinct mustelid carnivorans. *Zoological Journal of the Linnean Society* **150:** 895–914.

Sheffield SR, Thomas HH. 1997. Mustela frenata. *Mammalian Species* **570**: 1–9.

Slater GJ, Harmon LJ, Alfaro ME. 2012. Integrating fossils with molecular phylogenies improves inference of trait evolution. *Evolution* **66:** 3931–3944.

Stayton CT. 2006. Testing hypotheses of convergence with multivariate data: morphological and functional convergence among herbivorous lizards. *Evolution* **60:** 824–841.

Stayton CT. 2014. convevol: uantifies and assesses the significance of convergent evolution. *R package*. https://cran.r-project.org/web/packages/convevol/

Stayton CT. 2015. The definition, recognition, and interpretation of convergent evolution, and two new measures for quantifying and assessing the significance of convergence. *Evolution* **69:** 2140–2153.

Tarasoff F. 1972. Comparative aspects of the hind limbs of the river otter, sea otter and seals. *Functional Anatomy of Marine Mammals* **1:** 333–359.

Taylor ME. 1989. Locomotor adaptations by carnivores. In: Gittleman JL , eds. *Carnivore behavior, ecology, and evolution*. Ithaca, NY: Springer, 382–409.

Van Valkenburgh B. 2007. Deja vu: the evolution of feeding morphologies in the Carnivora. *Integrative and Comparative Biology* **47:** 147–163.

Wiley DF, Amenta N, Alcantara DA, Ghosh D, Kil YJ, Delson E, Harcourt-Smith W, Rohlf FJ, St John K, Hammann B. 2005. Evolutionary morphing. In: *Visualization, 2005. VIS 05.* IEEE. Minneapolis: IEEE, 431–438.

Williams TM. 1983a. Locomotion in the North American mink, a semi-aquatic mammal. II. The effect of an elongate body on running energetics and gait patterns. *The Journal of Experimental Biology* **105:** 283–295.

Williams TM. 1983b. Locomotion in the North American mink, a semi-aquatic mammal. I. Swimming energetics and body drag. *The Journal of Experimental Biology* **103:** 155–168.

Williams TM. 1986. Thermoregulation of the North American mink during rest and activity in the aquatic environment. *Physiological Zoology* **59**: 293–305.

Wroe S, Milne N. 2007. Convergence and remarkably consistent constraint in the evolution of carnivore skull shape. *Evolution* **61:** 1251–1260.

Youngman PM. 1990. Mustela lutreola. *Mammalian Species* **362**: 1–3.

SUPPORTING INFORMATION

Additional Supporting Information may be found in the online version of this article at the publisher's website:

Figure S1. Test of measurement repeatability for the forelimb long bones. (A, C, E): PCA of measurement repetition; (B, D, F): neighbour joining tree of the inter-measurement Euclidean distances in the tangent space; A, B: humerus; C, D: ulna; E, F: radius.

Figure S2. Test of measurement repeatability for the hind-limb long bones. (A, C, E): PCA of measurement repetition; (B, D, F): neighbour joining tree of the inter-measurement Euclidean distances in the tangent space; A, B: femur; C, D: tibia; E, F: fibula.

Figure S3. Neighbour joining trees computed on Euclidean distances between species coordinates in the tangent space. A: humerus; B: ulna; C: radius; D: femur; E: tibia; F: fibula. Bold: mink species.

Table S1. Convergence metrics and associated *P*-values for each bone for the two minks (*Mustela lutreola* and *Neovison vison*), and each mink versus the Lutrinae common ancestor (ancestral state reconstruction) computed on the residuals of the multivariate regression of the shape on the Log_{10} of the body mass. Bold: significant.